Catal Lett (2016) 146:483–492
DOI 10.1007/s10562-015-1664-7

Selective Oxidation of Methane to Methanol Over Cu- and Fe-Exchanged Zeolites: The Effect of Si/Al Molar Ratio

Christos Kalamaras[1] · David Palomas[2] · Rene Bos[3] · Andrew Horton[3] · Mark Crimmin[2] · Klaus Hellgardt[1]

Received: 1 October 2015 / Accepted: 17 November 2015 / Published online: 27 January 2016

Abstract A series of Cu-, Fe- and Fe/Cu-containing zeolite (ZSM-5, beta, Y) catalysts were prepared to investigate the effect of zeolite's physicochemical properties on the total oxygenates production and MeOH selectivity from the partial methane oxidation using H_2O_2 as oxidizing agent. The NH_3-TPD studies have shown that the zeolite type and Si/Al molar ratio are correlated with the acid sites strength and concentration. The latter surface property was proved to have a strong influence on the oxygenate productivity. In particular, a significant increase of the methanol production was observed when lowering Si/Al ratio in the ZSM-5, Fe/ZSM-5, Cu/ZSM-5 and Cu–Fe/ZSM-5 catalysts. This can be explained by the increased amount of Brønsted acid sites capable of accommodating the active catalyst (Fe species). The Fe-only ZSM-5 catalysts exhibited the highest catalytic activity (total oxygenated products) with HCOOH being the major product, whereas the presence of only Cu was found to suppress the production of MeOOH and HCOOH. On contrary, the deposition of both Fe^{3+} and Cu^{2+} results to a switch in selectivity and the target product, MeOH, was observed in ~80 % selectivity. In the case of Cu-only ZSM-5 catalysts, a similar activity to methanol was observed regardless the copper source and synthesis method. The activity/selectivity findings of the present study confirm and complement the conclusions of the previous work by Hammond et al. (ACS Catal 3:689, 2013; ACS Catal 3:1835, 2013; Angew Chem Int Ed 51:5129, 2012; Chem Eur J 18:15735, 2012) over the well-studied Cu–Fe–zeolite system, providing also complete material balance based on both gas and liquid reaction products.

Graphical Abstract

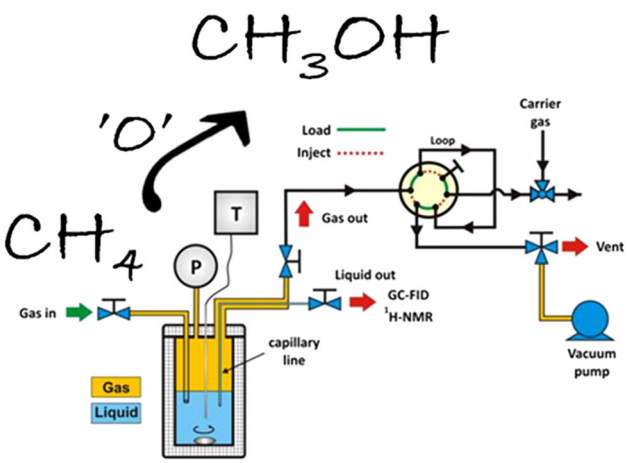

Keywords Partial oxidation of methane · ZSM-5 zeolite · Acidity · Methanol production

✉ Klaus Hellgardt
k.hellgardt@imperial.ac.uk

[1] Chemical Engineering Department, Imperial College London, South Kensington, London SW7 2AZ, UK

[2] Chemistry Department, Imperial College London, South Kensington, London SW7 2AZ, UK

[3] Emerging Technologies, Shell Global Solutions International B.V., P.O. Box 38000, 1030 BN Amsterdam, The Netherlands

1 Introduction

The efficient and selective oxidation of methane to methanol remains a challenging problem for catalytic science and if solved would have the potential to revolutionize the petrochemical industry. The conversion of methane to

energy-dense liquid derivatives, such as methanol, could lead to significant breakthroughs in the utilization of natural gas as a primary feedstock [5]. Presently, methanol production is an energy-intensive two-stage process involving the intermediate manufacture of synthesis gas [6]. This technology is potentially not economically viable in remote regions where a significant fraction of the world's reserves of methane are found [7].Therefore, there is significant interest in the valorization of methane in a single and preferentially non-energy-intensive step to facilitate its utilization on an industrial scale.

Despite decades of research in the field of C–H activation, due to the large single bond enthalpy of 438.8 kJ mol^{-1}, low polarisability and low solubility of methane the problem of selective and catalytic methane to methanol oxidation still remains unsolved [8]. Due to facile over-oxidation of methanol, the design of a catalytic system that not only activates methane, but is able to do so under intrinsically mild reaction conditions is required. Three main approaches have been reported, namely: (i) direct high temperature-high pressure activation of alkanes in low yield but high selectivity processes [9–11], (ii) oxidation in strong acidic media using noble metal catalysts to produce alcohol derivatives as esters [12–15], and (iii) activation under moderate conditions using micro/mesoporous catalysts containing transition metal sites and N_2O/O_2 which operate without catalytic turnover [16–21].

In nature, methane monooxygebase (MMO) uses dioxygen from air, in combination with 2 protons and 2 electrons, as the terminal oxidant for a highly selective, one-step methane oxidation that operates at room temperature and atmospheric pressure [22]. While biomimetic catalysts based upon the di-iron active site of soluble MMO (sMMO) have been investigated extensively for alkane oxidation, the active di-copper site of particulate MMO (pMMO) was only elucidated in 2010 [23–26]. Recently, a novel low-temperature selective oxidation of methane to oxygenated products in aqueous phase using hydrogen peroxide as the oxidant over Cu- and Fe-containing mordenite framework inverted (MFI)-type zeolites was reported [1–4, 27]. The authors demonstrated that the reaction proceeds through a methyl hydroperoxide (MeOOH) intermediate, which subsequently converts to methanol (MeOH) with high yield and selectivity in a closed catalytic cycle. However, some overoxidation to formic acid (HCOOH) and CO_2 was also observed at various levels of selectivity. The active sites were attributed to trace impurities of iron, which is proposed to exist as extra-framework diiron–μ-oxo-hydroxo complexes or oligomeric iron complexes within the zeolite micropores [1–4, 27]. The addition of Cu^{2+} appears to militate against methanol over-oxidation processes, leading to binary Cu–Fe/ZSM-5 catalysts capable of very high selectivity towards methanol [1–4, 27]. Based on EPR radical trapping studies, the authors proved that Cu ions are able to control the production of hydroxyl radicals, which facilitate the over-oxidation of methanol to formic acid. It is noteworthy that the developed catalyst was found to be over 3 orders of magnitude more active than any previously reported system for direct methane oxidation.

In this contribution, we investigate the effect and role of the Si/Al ratio of the ZSM-5 support on the activity and selectivity of Cu–Fe/ZSM-5 catalysts in the partial oxidation of methane to methanol. We show that the Si/Al ratio and in particular the resulting acidity of the support has a significant effect on catalytic activity. We propose that this effect is due to an increase in the amount of Brønsted acid sites, which are capable to accommodate the active extra-framework Fe species.

2 Experimental

2.1 Catalyst Synthesis

Two common techniques were employed for the synthesis of M/zeolite (where, M = Fe and/or Cu) type catalysts.

i. Catalysts were prepared by Solid State Ion Exchange (SSIE) technique in order to introduce Fe and/or Cu metals into various zeolite structures (i.e. ZSM-5, beta, Y) using different Cu(II) and Fe(III) precursors, namely acetylacetonate (acac), chloride and nitrate. The synthesis procedure involved the following steps: $[Fe(acac)_3]$ was added to the desired amount of the ammonium form of ZSM-5 zeolite and ground in a pestle and mortar for 30 min. The catalysts were subsequently activated prior to use, by calcination at 550 °C (10 °C min^{-1}) for 3 h in static air. This protocol was used to prepare all Cu-only, Fe-only and Fe–Cu bimetallic exchanged-zeolites using the appropriate amount of copper(II) and/or iron(III) precursors.
ii. The wet impregnation (WI) technique was used as an alternative method for the preparation of Cu-only zeolite (ZSM-5, SiO_2/Al_2O_3 = 30) catalysts in order to probe the influence of the synthesis route on the activity and selectivity of the prepared catalysts. The Cu(II) zeolite-supported catalysts were prepared by impregnating the ammonium form of ZSM-5(30) with a given amount of aqueous precursor solution (i.e. $Cu(acac)_2$, $CuCl_2$, $Cu(NO_3)_2{\cdot}3H_2O$) corresponding to the desired 2.5 wt% Cu loading. After gradual evaporation of water at 70 °C for 4 h, the resulting solid was then dried at 120 °C overnight and then calcined at 550 °C (10 °C min^{-1}) for 3 h in static air.

All the ZSM-5 (SiO_2/Al_2O_3 = 23, 30 and 80) and beta (SiO_2/Al_2O_3 = 25) zeolites were purchased from Zeolyst® International in the ammonium form. The ammonium Y zeolite (SiO_2/Al_2O_3 = 5) was sourced from Sigma Aldrich. The number in parenthesis after each zeolite indicates the nominal SiO_2/Al_2O_3 molar ratio.

2.2 Physicochemical Characterization

The specific surface area (SSA, $m^2\ g^{-1}$) of the commercial zeolites was determined by applying the BET method. N_2 adsorption/desorption isotherms obtained at 77 K over the entire range of relative pressures on samples previously outgassed at 300 °C for 2 h (Micromeritics TriStar 3000 analyser) were used to estimate the pore volume (V_p, $cm^3\ g^{-1}$) of the solids. X-ray Fluorescence (XRF) chemical analysis was performed at room temperature on a Bruker S4EXPLORER apparatus in order to determinate the SiO_2/Al_2O_3 molar ratio of the commercial zeolites. Approximately 1 g of each powder sample was placed into a 40 mm sample cup mounted with 4 μm polypropylene film and analyzed by XRF.

X-Ray diffraction was used for phase identification, and to probe: (i) the presence of Fe and/or Cu X-ray active oxides in the zeolite, and (ii) the influence of the synthesis method, SiO_2/Al_2O_3 ratio and precursor materials on the morphology and crystallinity of the final catalysts. Powder X-ray diffraction patterns of the prepared solids were recorded in the 5–75° 2θ range (PANalytical X'Pert PRO diffractometer using Cu Kα radiation, λ = 1.5418 Å) with a step scan of 0.2° min^{-1}.

The Al, Fe, Cu and Na content of the commercial zeolites was determined by ICP-OES (Perkin–Elmer 2000 DV ICP-OE spectrometer). Each zeolite was analyzed after calcination of the commercial source (ammonium form) for 2 h under static air at 550 °C. Approximately 0.1 g of the commercial zeolite was weighed accurately and digested with 0.5 mL of concentrated hydrofluoric acid (48 %) by heating at 100 °C for 30 min. After evaporating the acid, 0.25 mL each of concentrated nitric acid (68 %) and concentrated hydrochloric acid (37 %) were added and digestion continued for another 30 min. This was diluted to 5 mL with deionized water, and 2 mL of boric acid (2 %) and was further diluted as needed with 2 M nitric acid prior to analysis (3 mL in 25 mL of total volume).

The acidity of the prepared M/ZSM-5(30) catalysts as well as that of the H-form of all zeolites investigated was determined by NH_3-Temperature Programed Desorption (TPD) technique. All NH_3-TPD experiments were carried out in a conventional flow-through quartz reactor with helium as carrier gas (50 mL min^{-1}). Typically, 200 mg of sample was pretreated by heating in a flowing stream of helium from 25 to 550 °C (10 °C min^{-1}). This was done to remove water and impurities. The temperature was held at 550 °C for 1 h and then cooled to 100 °C under flowing gas (He). Then, the He flow was switched to 10 vol% NH_3/He for 30 min. Following this the reactor was purged with He for a further 1 h to remove weakly adsorbed NH_3. A linear temperature program of 5 °C min^{-1} was used to follow the desorption of NH_3 (m/z = 17) with evolved gas detected by a quadrupole mass spectrometer (PFEIFFER Vacuum, ThermoStar™).

2.3 Methane to Methanol Reaction

All catalytic tests for the oxidation of methane were carried out with H_2O_2 over a custom-made batch apparatus shown in Fig. 1. The stainless-steel autoclave (50 mL) reactor containing a Teflon® liner and a Teflon® coated magnetic stirrer was charged with an aqueous solution of H_2O_2 (10 mL, 0.5 M) and the desired amount of catalyst (27 mg). After sealing, the reactor was charged with CH_4 to a fixed pressure (30.5 bar) after a series of purges (5 times) to remove permanent gases. This is equivalent to 36 mmol of CH_4 in the gas phase. The autoclave was heated to the reaction temperature (50 °C), and vigorously stirred at 1500 rpm once the desired temperature was obtained. After a reaction time of 30 min, a gas sample loop (0.5 mL) was filled with product gas from the exit of the reactor and injected via a 6-way chromatographic valve with electrical actuator to a mass spectrometer (European Spectrometry System II) for analysis using a constant flow of carrier gas (Ar, 300 mL min^{-1}). The mass numbers (m/z), 15 (CH_3^+), 16 (CH_4), 18 (H_2O), 28 (CO), 31 (CH_3O^+), 32 (O_2) and 44 (CO_2) were continuously monitored using Quadstar 32bit software. The purity of the gases used (CH_4, CO_2, Ar, provided by BOC gases UK) was greater than 99.95 vol%. The amount of CO_2 in the product gas (μmol) was calculated by multiplying the area (ppm.s) of the CO_2 molar fraction signal with the carrier gas flow rate (mol s^{-1}). The vessel was subsequently cooled in an ice bath to 12 °C in order to reduce volatility of any liquid products that may have formed. The liquid product solution was then filtered and samples were analyzed by an Agilent 6890 GC equipped with FID detector and ^{1}H-NMR spectroscopy.^{1}H NMR spectra were measured at a frequency of 500.13 MHz using a Bruker AVANCE III HD 500 spectrometer operating at 298 K. Solvent suppression (HOD), along with ^{13}C decoupling to remove ^{13}C satellite signals, were achieved using the pulse program wetdc [28]. All relevant parameters were selected automatically via execution of the Bruker AU program au_lc1d after obtaining a ^{1}H spectrum showing the solvent chemical shifts.

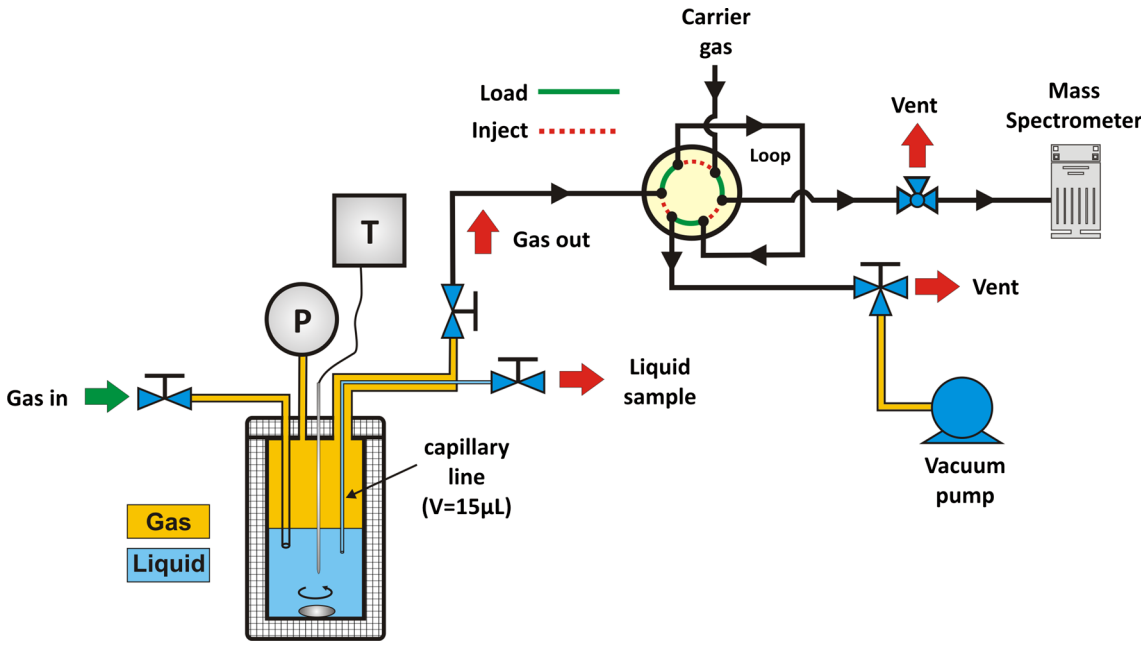

Fig. 1 Experimental set-up used for the aqueous-phase selective oxidation of methane to methanol by H_2O_2

3 Results and Discussion

3.1 Catalyst Characterization

Table 1 lists the physical properties and chemical composition of the commercial zeolites investigated. It is clear that the beta zeolite exhibits the highest specific surface area and pore volume of all commercial zeolites studied. For the ZSM-5 zeolites the specific surface area and pore volume slightly increases with increasing Si/Al molar ratio. Elemental analysis of the commercial materials was performed in order to determine the role played by any potential metal impurities within the structure. The ICP results shown in Table 1 revealed that each sample contained trace amounts of the transition metals Fe and Cu. In the case of the ZSM-5 series and beta zeolites trace amounts of Na were also observed. The results are in line with relevant MSDS sheets indicating a residual 0.05 wt% Na_2O content. In the case of the Y-type zeolite the Na content was equivalent to 4 wt% Na_2O. Moreover, in all cases the SiO_2/Al_2O_3 molar ratios reported by the manufacture (number in parenthesis) are in good agreement with the XRF analysis.

X-ray diffraction patterns of the M/ZSM-5(30) and M/beta (where, M = Fe or Cu) solids prepared by SSIE using acetylacetonate precursors, are presented in Fig. 2. It is observed that both Cu- and Fe-exchanged catalysts maintained the MFI and BEA framework structure of ZSM-5 and beta zeolite, respectively [29]. Moreover, no shift of the main diffraction peaks of the 2.5 wt% metal containing materials was noticed with respect to the protonated zeolites. The latter experiment indicates no shrinkage/expansion of the crystal lattice due to introduction of Cu^{2+} and Fe^{3+} into the zeolite framework. Similar to the work of Hammond et al. [1], it is suggested that the framework metal cations formed by hydrothermal synthesis

Table 1 Physical properties, elemental analysis and SiO_2/Al_2O_3 molar ratios of the commercial zeolites investigated

Zeolite	SSA[a] (m^2 g^{-1})	V_p^a (cm^3 g^{-1})	Al[b] (ppm)	Fe[b] (ppm)	Na[b] (ppm)	Cu[b] (ppm)	$SiO_2/Al_2O_3^c$
ZSM-5(23)	384	0.209	21,571	233	270	14	25.7
ZSM-5(30)	363	0.223	19,502	179	123	1	35.7
ZSM-5(80)	439	0.264	8391	204	214	4	94.0
beta(25)	601	0.687	23,102	219	156	2	27.4
Y-zeolite(5)	430	0.220	105,786	190	16,047	1	–

[a] Determined by BET method

[b] Determined by ICP-OES

[c] Determined by XRF

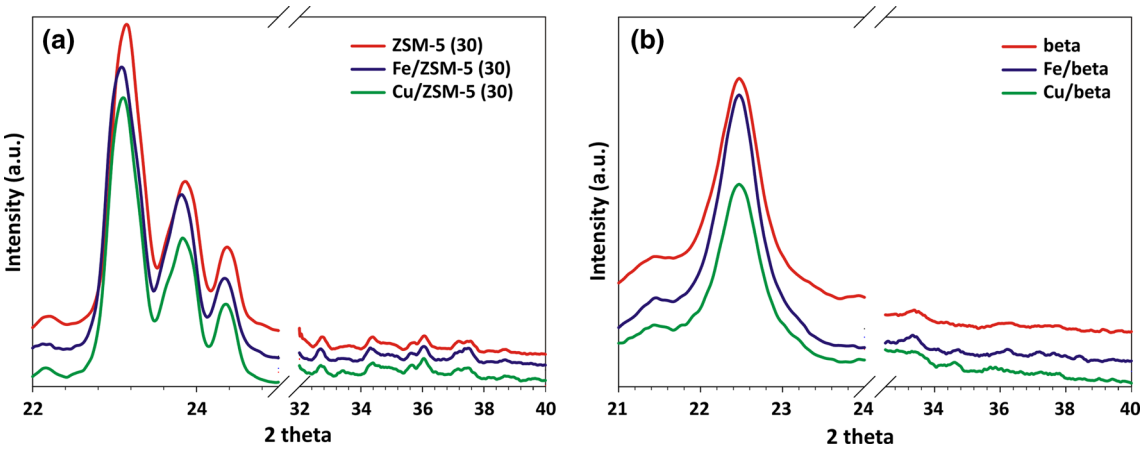

Fig. 2 Powder XRD patterns of the **a** M/ZSM-5(30) and **b** M/beta (where, M = Fe or Cu) catalysts in the 22–40° 2θ range

are able to migrate to the extra-framework during heat pretreatment. While for Fe-exchanged zeolites several iron oxide phases could be formed, including hematite (α-Fe_2O_3), maghemite (γ-Fe_2O_3), lepidocrocite (γ-FeO–OH), gohetite (α-FeO–OH), wustite (FeO) and magnetite (Fe_3O_4) [30], after careful analysis none of these phases were detected (Fig. 2).

Figure 3 shows the XRD patterns of the Cu/ZSM-5(30) solids prepared by WI and SSIE synthesis methods, derived from $CuCl_2$, $Cu(NO_3)_2{\cdot}3H_2O$ and $Cu(acac)_2$ precursors. Near identical diffraction patterns were observed for all Cu-containing samples, indicative only of the MFI structure with no evidence of segregation of the CuO phase. CuO has the most intense diffraction lines at 2θ values of 35.6 and 38.7°. Despite these observations, CuO [31] was detected in ZSM-5-containing zeolites when the transition metal content exceeded 5 %. One may argue simply that metal oxide aggregates, larger than 5 nm particle size, are not present in the various Cu/ZSM-5(30) catalysts, since XRD is a bulk sensitive technique that requires crystallites of minimum dimensions near 5 nm. According to literature [32], at least three types of copper species have been proposed for Cu-exchanged zeolites: (i) isolated ions interacting with the framework Al, either without an extra framework ligand, or with an extra framework O or OH ligand, (ii) polymeric chains or multinuclear species (often referred to as small copper–oxygen aggregates, for instance $[Cu–O–Cu]^{2+}$ inside the channels, and (iii) oxide particles on the external surface of zeolite. Our data suggest that independent of the synthesis method and precursor material used, Cu^{2+} ions are well dispersed in the framework while the structure is globally maintained. This would explain the similar methanol yield observed for these catalysts under selective methane oxidation conditions using H_2O_2 (see Sect. 3.3; Table 4).

The Cu and Fe content of the final solids (M/zeolite, where M = Cu and/or Fe) after SSIE was also determined by ICP. Elemental analysis of the resulting materials after

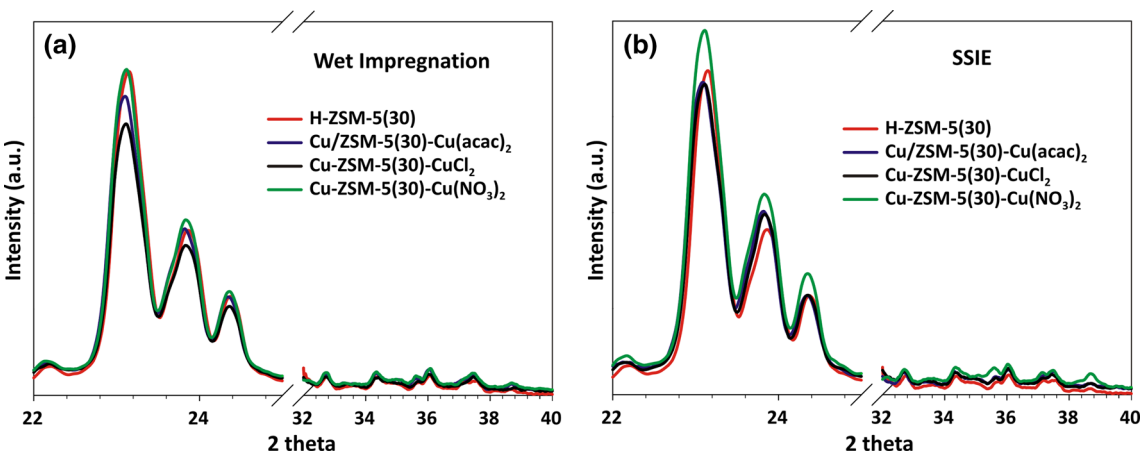

Fig. 3 Powder X-ray diffraction patterns of the Cu/ZSM-5(30) solids prepared by **a** WI and **b** SSIE method, derived from various Cu(II) precursors in the 22–40° 2θ range

calcination for 3 h under static air at 550 °C was performed in order to probe the exchange capacity of the metal (Fe and/or Cu) into the zeolite structure. The results shown in Table 2 revealed that in both Fe- and Cu-exchanged zeolites, the materials were found to contain more than 85 % of the nominal values of the transition metals (Fe and Cu). In the present study the actual form of Fe and Cu metal into the zeolites was not identified.

3.2 Acidity Studies by NH_3-Temperature Programmed Desorption (TPD)

In the TPD of ammonia, the strength of the NH_3 interaction with acid sites is reflected in the temperature profile of the desorption rate. The area under the peaks is proportional to the total number of acid sites in the catalyst under study. The absolute number of acid sites was quantified by multiplying the area of the peak with the feed gas flow rate. The NH_3 desorption profiles during TPD for ZSM-5(30), Cu/ZSM-5(30) and Fe/ZSM-5(30) catalysts are shown in Fig. 4 and the total amounts of desorbed NH_3 (μmol g^{-1}) and the peak maxima (T^{i}_{max}) are given in Table 3.

As shown in Fig. 4, the M/ZSM-5(30) catalysts exhibited different profiles compared to the parent material. Two major desorption events were noted for H-ZSM-5(30) with maxima at 197 and 409 °C indicating the presence of weak and strong acid sites, respectively. In particular, the peak observed at 197 °C is caused by weakly physisorbed and coordinated NH_3 on Lewis acid sites, while the peak at about 409 °C is related to NH_4^+ ions with three hydrogen atoms bonded to three oxygen ions of AlO_4 tetrahedra (3H structure) on Brønsted acid sites [33–36]. The incorporation of Cu and Fe metal ions into ZSM-5(30) results in a decrease of the total acidity of the zeolite as measured by a lower amount of NH_3 desorbed. In the case of Fe-exchanged ZSM-5(30), the NH_3 desorption peak at 409 °C decreased significantly (see Fig. 4; Table 3), indicating a reduction of Brønsted acidity, which suggests that the Brønsted acid protons of ZSM-5 were substituted by Fe^{3+}.

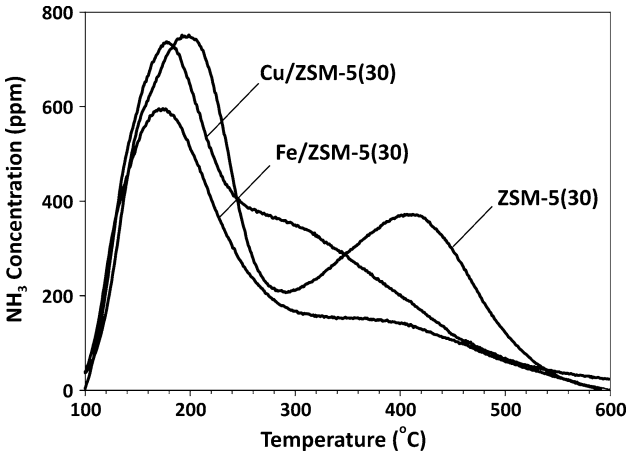

Fig. 4 NH_3-TPD profiles obtained over ZSM-5(30), Cu/ZSM-5(30) and Fe/ZSM-5 catalysts prepared by SSIE method

Table 3 Total amount of desorbed NH_3 and peak maximum during TPD experiments

Catalyst	NH_3 (μmol g^{-1})	T^{1}_{max} (°C)	T^{2}_{max} (°C)
ZSM-5(23)	894	188	411
ZSM-5(30)	613	185	400
Cu/ZSM-5(30)	613	174	315
Fe/ZSM-5(30)	452	175	403
ZSM-5(80)	354	176	370
Beta(25)	347	168	320

This explanation is also supported by previous work of Long et al. [34] by a separate NH_3-TPD experiment over NH_4-ZSM-5 where no NH_3 desorption peak near 160 °C was seen, but a peak at 390 °C was observed. On the other hand, incorporation of Cu into the ZSM-5(30) created weak acid sites, as indicated by NH_3 desorption below 400 °C. NH_3 desorption from Cu/zeolite between the range 250–300 °C was correlated to NH_3 desorption occurring from Cu–NH_3 complex [37].

Table 2 Cu and Fe content of the final solids after SSIE as determined by ICP

Final catalyst	SiO_2/Al_2O_3	Cu (wt %)	Fe (wt %)
2.5 wt% Cu/ZSM-5	30	2.23	0.02
2.5 wt% Fe/ZSM-5		0.003	2.16
1.25 wt% Cu/1.25 wt% Fe/ZSM-5		1.11	1.01
2.5 wt% Cu/ZSM-5	23	2.64	0.05
2.5 wt% Fe/ZSM-5		0.003	2.79
1.25 wt% Cu/1.25 wt% Fe/ZSM-5		1.35	1.32
2.5 wt% Cu/beta	25	2.90	0.04
2.5 wt% Fe/beta		0.0003	2.92
1.25 wt% Cu/1.25 wt% Fe/beta		1.48	1.48

The total acidity of the beta and ZSM-5 zeolites with different Si/Al molar ratios was also determined by the NH_3-TPD technique. Figure 5 shows the typical acid site distribution as obtained by NH_3-TPD. Similar to Fig. 4, all zeolites exhibited two well resolved desorption peaks: the low-temperature peak (LTP) at 176–188 °C and the high-temperature peak (HTP) at 320–411 °C. It was found that the HTP increased as the Si/Al ratio decreased in the case of ZSM-5 zeolites, whereas the beta zeolite showed the lowest NH_3 desorption temperature. Figure 5 also shows that the desorption temperature of ammonia from the strong acid sites shifted to higher temperature as the Si/Al ratio decreased, strongly suggesting the existence of aluminum in extra-framework positions. The total amount of NH_3 adsorbed onto weak and strong acid sites of beta and ZSM-5 with different molar ratio of Si/Al is shown in Table 3. It is clearly seen that the total acid sites of ZSM-5 decrease with increasing of Si/Al molar ratio, data which agree well with those reported in the literature [38, 39]. The results show that the zeolite type and the molar ratio of Si/Al have a significant effect on the physicochemical properties of the final catalysts.

Costa et al. [38, 40, 41] suggested that the strength and concentration of the acid sites could be quantitatively correlated with the activity for the catalytic cracking of *n*-heptane and light olefins in a variety of Y and ZSM-5 zeolites. In these studies, it was verified that acid catalyzed reactions over zeolites could be described by Brønsted-type relations. Beyond the determinant factor of framework composition of the zeolites, the spatial distribution of acid sites across the framework is also important, i.e., for a given composition, the structure type will modify the surface properties [42, 43].

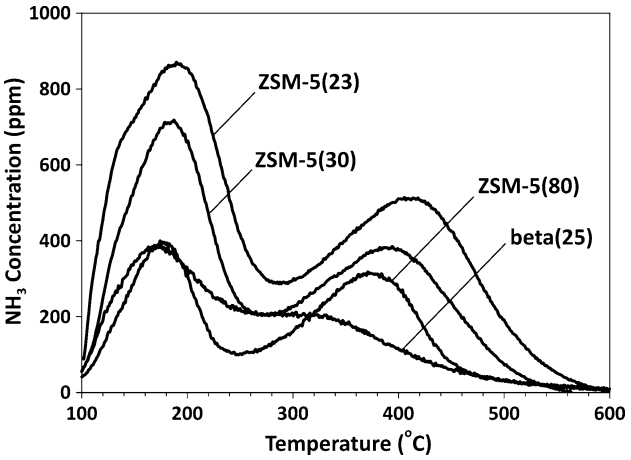

Fig. 5 NH_3-TPD profiles obtained over beta and ZSM-5 zeolites with different SiO_2/Al_2O_3 ratio

3.3 Catalytic Activity of Zeolite Based Catalysts

The metal catalysts prepared were tested for the selective oxidation of methane to methanol in an indirect process using H_2O_2 as oxidizing agent according to the experimental procedure described in Sect. 2.3. The catalytic evaluation tests were conducted on the prepared solids as a function of: (i) the synthesis method and Cu precursor (Table 4), and (ii) the SiO_2/Al_2O_3 molar ratio and zeolite type (Table 5).

As shown in Table 4, the protonated and Fe-only ZSM-5(30) zeolites (entries 1 and 2, Table 4) exhibited comparable methanol yields with those reported by Hammond et al. [3] under the same experimental conditions. On the other hand, the Cu-only and bimetallic Fe–Cu catalysts (entries 3–9, Table 4) were found to give lower (65–75 %) yields of methanol compared with the literature value. Initially it was thought that this may be due to the choice of precursor material, however, it was found that the preparation method and the Cu precursor have only minor effects on the total methanol production. Based on the physicochemical characterization of the Cu-containing catalysts, a similar structure was obtained despite different synthesis methods and Cu precursors, while >90 % of Cu^{2+} cations were introduced into zeolite pore (Table 2) after SSIE.

The results of Table 5 indicate that the zeolite type and Si/Al molar ratio have a strong influence on the methanol yield, since the Cu- and Fe-containing ZSM-5 zeolites ($SiO_2/Al_2O_3 = 23$) showed much higher activity in terms of methanol yield compared with the other catalysts investigated. According to Hammond et al. [1, 3], the level of activity exhibited by ZSM-5 for methane activation has proven so far to be unique. It was initially suggested that the enhanced activity could be attributed to: (i) the arrangement of molecular-sized pores and cavities found in the zeolite framework, which allows discrimination between molecules simply by size [44], (ii) a molecular confinement effect within the zeolite micropores, leading to increased interactions between confined reactants and allowing unusual transition states to be accessed [45, 46]. Alternative zeolites (i.e., y-zeolite, silicalite) with similar surface areas and pore structures were found to be far less active, suggesting that the confinement effect of the MFI framework alone does not explain the observed activity of the ZSM-5(23) zeolite.

The other possible explanation for the superior activity of ZSM-5 is the presence of Fe metal impurities. It was reported that even trace Fe concentrations within the MFI structure are capable to both activate hydrogen peroxide [47, 48] and catalyze various selective oxidations using H_2O_2 [1–4] and N_2O [49–51] as oxidizing agents. Indeed, elemental analysis of all commercial zeolites studied here demonstrated that in addition to the expected quantities of

Table 4 The effect of synthesis method and Cu precursor on methanol production with ZSM-5 zeolites

Entry	Catalyst	Synthesis method	Precursor	MeOH[a] (μmol)	Ref. [3] (μmol)
1	ZSM-5(30)	–	–	9.4	15.4
2	Fe/ZSM-5(30)	SSIE	$Fe(acac)_3$	29.2	19.6
3	Cu–Fe/ZSM-5(30)	SSIE	$Fe(acac)_3$; $Cu(acac)_2$	52.0	188.8
4	Cu/ZSM-5(30)	SSIE	$Cu(acac)_2$	20.2	65.3
5			$Cu(NO_3)_2$	29.7	
6			$CuCl_2$	21.7	
7		WI	$Cu(acac)_2$	14.4	
8			$Cu(NO_3)_2$	24.5	
9			$CuCl_2$	29.3	

[a] *Reaction conditions*: t = 30 min; T = 50 °C; P = 30.5 bar; $[H_2O_2]_o$ = 0.5 M; catalyst = 27 mg; rpm = 1500; V = 10 mL

Table 5 The effect of SiO_2/Al_2O_3 molar ratio and zeolite type on methanol production

Entry	Catalyst	SiO_2/Al_2O_3	MeOH (μmol)[a]	Ref. [3]
1	ZSM-5	23	16.8	15.4
2		30	9.4	
3		80	4.5	
4	beta	25	2.0	
5	Y-zeolite	5	2.1	
6	Fe/ZSM-5	23	47.7	19.6
7		30	29.2	
8		80	10.4	
9	Fe/beta	25	2.9	
10	Fe/Y-zeolite	5	4.0	
11	Cu/ZSM-5	23	47.4	65.3
12		30	20.2	
13		80	6.0	
14	Cu/beta	25	2.4	
15	Cu/Y-zeolite	5	3.1	
16	Cu–Fe/ZSM-5	23	126.3	188.8
17		30	52.0	
18		80	8.5	
19	Cu–Fe/beta	25	2.6	
20	Cu–Fe/Y-zeolite	5	4.9	

[a] *Reaction conditions*: t = 30 min; T = 50 °C; P = 30.5 bar; $[H_2O_2]_o$ = 0.5 M; catalyst = 27 mg; rpm = 1500; V = 10 mL

Al, trace (~200 ppm) levels of Fe metal were present (Table 1). Thus, it is clear that the Fe content alone is not responsible for the significant differences in the final activity observed at similar catalyst compositions.

On the other hand, ZSM-5 zeolites are also well known as multifunctional materials possessing both Brønsted and Lewis acidity associated with the Al^{3+} content and hence the SiO_2/Al_2O_3 molar ratio. As discussed previously in Sect. 3.2, the amount of Al^{3+} is correlated to the acid site strength and concentration as observed by NH_3-TPD studies (Table 3). It could be suggested that the high activity of the Cu- and Fe-exchanged ZSM-5(23) for the selective oxidation of methane is correlated to the strength and concentration of the acid sites, which are capable of accommodating extra-framework Fe species. This strongly suggests that the presence of Al^{3+} in the MFI-framework is highly beneficial to the activity of the catalyst. However, the precise role of Al^{3+} is still the subject of much debate. For instance, Notte [52] has shown that extra-framework iron atom(s) in close vicinity to the framework acidic aluminum atoms constitute active catalytic centers for the one-step benzene to phenol reaction with N_2O. Similarly, it has been reported [53] that the Fe–O–Al extra framework mixed oxide formed after activation of Fe- and Al-containing MFI materials could also exhibit catalytic activity for the same reaction. Recently, Hammond et al. [2] based on catalytic measurements and spectroscopic investigations suggested that the incorporation of non-catalytic trivalent cations (e.g., Al^{3+} or Ga^{3+}) into the MFI-framework leads to an increased migration of framework Fe^{3+} to the extra-framework during heat pretreatment possibly stabilized by the AlO_4 tetrahedra. It is important to note that, the extra-framework Fe^{3+} species are suggested to be the active catalytic components for selective aqueous-phase methane oxidation [3].

Table 6 presents the full product distribution obtained over Cu- and Fe-containing ZSM-5(23) catalysts under the same reaction conditions presented in Tables 4 and 5, as determined by ^{1}H-NMR spectroscopy and mass spectrometry for the liquid (MeOH, MeOOH, HCOOH) and gas (CO_2) products, respectively. It is obvious that the introduction of Fe cations into ZSM-5(23) leads to a significant increase in catalytic activity (total oxygenated products), although HCOOH becomes the major product with selectivity greater than 75 %. The presence of Cu cations was found to suppress the production of MeOOH and HCOOH, with an insignificant amount of CO_2 observed. It was noted

Table 6 Product distribution obtain over M/ZSM-5(23) catalysts (where, M = Fe and/or Cu)

Catalyst	MeOH[a] (μmol)	MeOOH[a] (μmol)	HCOOH[a] (μmol)	CO_2^b (μmol)	Total (μmol)	MeOH Selectivity (%)
ZSM-5(23)	14.0	13.7	3.8	3	34.5	40.6
Cu/ZSM-5(23)	17.1	–	–	6	23.1	74.0
Fe/ZSM-5(23)	17.9	2.3	88.0	34	142.2	12.6
Cu–Fe/ZSM-5(23)	135.0	–	–	38.5	173.5	77.8

[a] Analyzed by ^{1}H-NMR

[b] Determined by MS

that deposition of both Fe^{3+} and Cu^{2+} results in a switch in selectivity where HCOOH is no longer produced and the target product, MeOH, is observed at ~80 % selectivity. It is also worth noting, that in all cases, CO was not detected in the gas phase. Similar selectivity results were also observed by Hammond et al. [3] over Cu- and Fe-exchanged ZSM-5 with a molar SiO_2/Al_2O_3 of 30.

Based on previous studies [3, 4, 48] and the current data, the proposed reaction network for the oxidation of methane using H_2O_2 over ZSM-5 based catalysts is presented in Fig. 6. Broadly, methane oxidation proceeds by: (i) the catalytic activation of both hydrogen peroxide and methane to produce the primary reaction product, MeOOH, (route 1), (ii) subsequent decomposition or further reaction of MeOOH, leading to the formation of MeOH and HCOOH (routes 2 and 3), and (iii) production of CO_2 from over-oxidation (routes 4–7). Consequently, the results of Table 6 suggest that, although the inclusion of Cu^{2+} leads to a minor decrease in the total oxygenate productivity, it does result in the retention of methanol as the major product at a selectivity of 74 %. In the case of the Fe-containing ZSM-5(23), despite the catalyst being over four times more active than the ZSM-5(23) alone, the HCOOH selectivity is extremely high. Since HCOOH is the deepest oxidation product before production of CO_2, the increased selectivity suggests that this compound is mainly formed by the over-oxidation of MeOOH and MeOH (routes 2 and 3). Moreover, a larger quantity of CO_2 is produced via the non-selective decomposition of the partial oxygenate intermediates (MeOOH, MeOH, HCOOH) to CO_2. Nevertheless, the direct formation of CO_2 from methane cannot be excluded (route 7). In contrast, the bimetallic Fe–Cu catalytic system was found to maintain both high activity and MeOH selectivity. As shown in Fig. 6 (route 3), the most preferred product, MeOH, can be oxidised towards HCOOH, under the reaction conditions employed, by further reaction with hydroxyl radicals, which are produced from the homolytic cleavage of the HO–OH bond. According to the recent work of Hammond and co-workers [1–4], the addition of Cu^{2+} to the catalytic system can suppress this route entirely by its ability to minimise the production of OH radicals. It was suggested that the crucial role of Cu is either to act as a catalytic hydroxyl radical scavenger, quenching or converting any ^{x}OH radicals produced to non-participative species, or to inhibit the ability of Fe^{3+} to produce ^{x}OH radicals in the first place by limiting the production of Fe^{2+}.

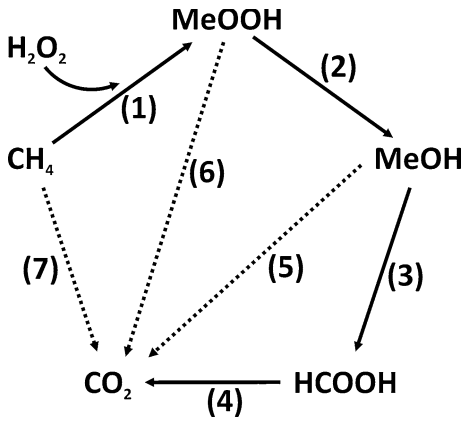

Fig. 6 Proposed reaction network for the oxidation of methane using H_2O_2 over ZSM-5 based catalysts. *Dashed lines* represent direct over-oxidation pathways

4 Conclusions

In the present work, it has been shown that the reactivity of commercial zeolite-based catalysts containing Fe and/or Cu cations for the partial oxidation of methane is related to the Si/Al molar ratio and type of zeolite, which is reflected by the acid sites strength and concentration. It was observed that the Cu-containing zeolites exhibited similar methanol yield under selective methane oxidation conditions, independent of synthesis method and Cu precursor material used. This could be explained by the formation and presence of similar CuO species. The bimetallic Cu–Fe/ZSM-5(23) catalyst was found to be the most efficient and selective catalyst for the oxidation of methane to methanol using H_2O_2 under mild reaction conditions

complementing the previous studies [1–4, 27]. It was suggested that the Fe cations are responsible for the superior oxygenates productivity, while the crucial role of Cu is to maintain high MeOH selectivity by suppressing the production of the deeper oxidation product, HCOOH.

Acknowledgments The financial support of the Royal Dutch Shell is gratefully acknowledged.

References

1. Hammond C, Dimitratos N, Jenkins RL, Lopez-Sanchez JA, Kondrat SA, Hasbi ab Rahim M, Forde MM, Thetford A, Taylor SH, Hagen H, Stangland EE, Kang JH, Moulijn JM, Willock DJ, Hutchings GJ (2013) ACS Catal 3:689
2. Hammond C, Dimitratos N, Lopez-Sanchez JA, Jenkins RL, Whiting G, Kondrat SA, ab Rahim MH, Forde MM, Thetford A, Hagen H, Stangland EE, Moulijn JM, Taylor SH, Willock DJ, Hutchings GJ (2013) ACS Catal 3:1835
3. Hammond C, Forde MM, ab Rahim MH, Thetford A, He Q, Jenkins RL, Dimitratos N, Lopez-Sanchez JA, Dummer NF, Murphy DM, Carley AF, Taylor SH, Willock DJ, Stangland EE, Kang J, Hagen H, Kiely CJ, Hutchings GJ (2012) Angew Chem Int Ed 51:5129
4. Hammond C, Jenkins RL, Dimitratos N, Lopez-Sanchez JA, ab Rahim MH, Forde MM, Thetford A, Murphy DM, Hagen H, Stangland EE, Moulijn JM, Taylor SH, Willock DJ, Hutchings GJ (2012) Chem Eur J 18:15735
5. Fiedler E, Grossmann G, Keresbohm DB, Weiss G, Witte C (2011) Ullmann's Encyclopaedia of Industrial Chemistry. Wiley-VCH, Weinheim
6. Twig MV, Bridger GW, Spencer MS (1989) Catalyst handbook, 2nd edn. Wolfe, London
7. Lunsford JH (2000) Catal Today 63:165
8. Schwarz H (2011) Angew Chem Int Ed 50:10096
9. Hunter NR, Gesser HD, Morton LA, Yarlagadda PS, Fung DPC (1990) Appl Catal 57:45
10. Foster NR (1985) Appl Catal 19:1
11. Gesser HD, Hunter NR, Prakash CB (1985) Chem Rev 85:235
12. Sen A (1998) Acc Chem Res 31:550
13. Periana RA, Taube DJ, Gamble S, Taube H, Satoh T, Fujii H (1998) Science 280:560
14. Aleksandr ES, Georgiy BS (1987) Russ Chem Rev 56:442
15. Shilov AE, Shul'pin GB (1997) Chem Rev 97:2879
16. Panov GI, Uriarte AK, Rodkin MA, Sobolev VI (1998) Catal Today 41:365
17. Knops-Gerrits PP, Goddard WA (2001) J Mol Catal A: Chem 166:135
18. Wood BR, Reimer JA, Bell AT, Janicke MT, Ott KC (2004) J Catal 225:300
19. Dubkov KA, Sobolev VI, Talsi EP, Rodkin MA, Watkins NH, Shteinman AA, Panov GI (1997) J Mol Catal A: Chem 123:155
20. Groothaert MH, Smeets PJ, Sels BF, Jacobs PA, Schoonheydt RA (2005) J Am Chem Soc 127:1394
21. Beznis NV, Van Laak ANC, Weckhuysen BM, Bitter JH (2011) Micro Meso Mater 138:176
22. Colby J, Stirling DI, Dalton H (1977) Biochem J 165:395
23. Bollinger JM Jr (2010) Nature 465:40
24. Balasubramanian R, Smith SM, Rawat S, Yatsunyk LA, Stemmler TL, Rosenzweig AC (2010) Nature 465:115
25. Hakemian AS, Rosenzweig AC (2007) Annu Rev Biochem 76:223
26. Martinho M, Choi DW, DiSpirito AA, Antholine WE, Semrau JD, Münck E (2007) J Am Chem Soc 129:15783
27. Forde MM, Armstrong RD, McVicker R, Wells PP, Dimitratos N, He Q, Lu L, Jenkins RL, Hammond C, Lopez-Sanchez JA, Kiely CJ, Hutchings GJ (2014) Chem Sci 5:3603
28. Smallcombe SH, Patt SL, Keifer PA (1995) J Magn Reson Ser A 117:295
29. Abu-Zied BM, Schwieger W, Unger A (2008) Appl Catal B: Environ 84:277
30. Qi G, Yang RT (2005) Appl Catal B: Environ 60:13
31. Nanba T, Masukawa S, Ogata A, Uchisawa J, Obuchi A (2005) Appl Catal B: Environ 61:288
32. Praliaud H, Mikhailenko S, Chajar Z, Primet M (1998) Appl Catal B: Environ 16:359
33. Brandenberger S, Kröcher O, Wokaun A, Tissler A, Althoff R (2009) J Catal 268:297
34. Long RQ, Yang RT (2001) J Catal 198:20
35. Akah A, Cundy C, Garforth A (2005) Appl Catal B: Environ 59:221
36. Sultana A, Sasaki M, Suzuki K, Hamada H (2013) Catal Commun 41:21
37. Flentge DR, Lunsford JH, Jacobs PA, Uytterhoeven JB (1975) J Phys Chem 79:354
38. Costa C, Dzikh IP, Lopes JM, Lemos F, Ribeiro FR (2000) J Mol Catal A: Chem 154:193
39. Shirazi L, Jamshidi E, Ghasemi MR (2008) Crys Res Tech 43:1300
40. Costa C, Lopes JM, Lemos F, Ramôa Ribeiro F (1997) Catal Lett 44:255
41. Costa C, Lopes JM, Lemos F, Ribeiro FR (1999) J Mol Catal A: Chem 144:233
42. Fajula F (1995) Stud Surf Sci Catal 97:133
43. Ribeiro FR, Alvarez F, Henriques C, Lemos F, Lopes JM, Ribeiro MF (1995) J Mol Catal A: Chem 96:245
44. Weisz PB (1980) Pure Appl Chem 52:2091
45. Corma A, García H, Sastre G, Viruela PM (1997) J Phys Chem B 101:4575
46. Sastre G, Corma A (2009) J Mol Catal A: Chem 305:3
47. Cavani F, Ballarini N, Luciani S (2009) Top Catal 52:935
48. Yuan Q, Deng W, Zhang Q, Wang Y (2007) Adv Synth Catal 349:1199
49. Cavani F, Teles JH (2009) ChemSusChem 2:508
50. Yuranov I, Bulushev DA, Renken A, Kiwi-Minsker L (2004) J Catal 227:138
51. Jia J, Sun Q, Wen B, Chen L, Sachtler WH (2002) Catal Lett 82:7
52. Notté P (2000) Top Catal 13:387
53. Hensen EJM, Zhu Q, Janssen RAJ, Magusin PCMM, Kooyman PJ, van Santen RA (2005) J Catal 233:123